INTERCONNECTION AND ENCAPSULATION OF INTEGRATED CIRCUITS BY ANODIC BONDING

Final Technical Report

Period Covered 1 July 1966 - 31 March 1967

Prepared For

NATIONAL AERONAUTICS AND SPACE ADMINISTRATION

Contract No. NAS 12-142

NASA

ELECTRONIC RESEARCH CENTER

575 Technology Square

Cambridge, Massachusetts 02139

Attn: CQ/Qualifications and Standards Laboratory

P. R. MALLORY & CO. INC.

Laboratory for Physical Science

Northwest Industrial Park

Burlington, Massachusetts 01803

TABLE OF CONTENTS

		Page
	Introduction	1
1.	Selection of Glass	4
2.	Metallization	4
3.	Geometrical Modifications	21
4.	Hermeticity	23
5.	Electrical Characteristics of Diodes	25
6.	Phosphorous Diffused Diodes	31
7.	Recommendations	34

INTRODUCTION

The object of this contract is to apply the Mallory proprietary bonding technique to the encapsulation via the flip chip approach of metallized silicon planar junctions. A sketch of the encapsulation scheme is shown in Figure 1. Typical planar diodes are provided with metallization consisting of a 5 mil wide line which terminates in a pad on each end. One pad contacts the diffused silicon. The other pad is positioned on the planar oxide. Above the diode is shown a sheet of glass with a matching metallization pattern. The glass sheet is bonded to the silicon diodes in such a way that the critical junction regions are hermetically covered by the glass and the metallizations on the glass and the diodes are aligned so that the diffused silicon regions may be electrically contacted by means of the metal pads on the glass. Bonding is accomplished at relatively low temperatures. No fluxes, adhesives or other intermediary materials are required and as used for the purposes of the contract work, metals and glass remain solid throughout the bonding procedure.

It should be appreciated that this packaging concept could easily be extended to more elaborate geometries. If it can be made to work for simple diodes it should also be suitable for transistors and monolithic circuits. Indeed, we can visualize a relatively large sheet of metallized

glass serving as a circuit board to which a number of individual devices or integrated circuit chips may be bonded.

Although the concept of this contract work is a version of the popular flip-chip approach, it differs from it in the following regard. In conventional flip-chip approaches the goal is merely electrical interconnection. By contrast, in our approach the goal is simultaneously to interconnect and to encapsulate hermetically.

One of the essential parameters in this work is the sealing temperature. If a glass could be found which permitted hermetic sealing at temperatures below 570^{o}C then it would be possible to use diodes with the conventional aluminum metallization. Accordingly, the first month of this contract was largely spent in a search for a low sealing glass. As described in section 1 this search proved to be unsuccessful. Hence, it became necessary to develop and evaluate a high temperature metallization. The necessary equipment was built and the metallization evaluated in the subsequent four contract months. This work is described in section 2.

During the fifth contract month we became aware of certain geometrical difficulties which required drastic modification as described in section 3. In the remaining months, the degree of hermeticity of the encapsulation was evaluated and work was done on the electrical

characteristics of the devices. These activities are described in sections 4 and 5.

Boron diffused p- on n- junctions were used in almost all of the contract work. Some very preliminary data on phosphorous diffused n- on p- junctions are reported in section 6. Finally, recommendations are presented in section 7.

Accomplishments of the project can be summarized as follows.

1. A metallization has been developed which meets the requirements of the sample geometry.
2. We have demonstrated that our bonding process is capable of producing diodes with excellent reverse characteristics.
3. A number of diodes have been made which have good forward characteristics.
4. Although the hermeticity problem has not been completely solved, in our best efforts about 97 percent of the critical junction periphery has been sealed hermetically.

This report summarizes six months' work carried out by 1 1/4 professionals and one technician over a nine months period.

1. SELECTION OF GLASS

In the selection of a suitable glass the following requirements had to be met.

1. It must be sealable by our process.
2. It should seal at as low a temperature as possible.
3. Its coefficient of thermal expansion should closely match the coefficient of silicon which approximately equals 3.2 x $10^{-6}/^{o}C$.
4. The glass should preferably have a low alkali content since alkali ions in the vicinity of the silicon surface are known to have an adverse effect on junction leakage.

With our technique most glasses can be bonded to flat silicon well below $500^{o}C$ and to flat oxidized silicon at temperatures above $550^{o}C$. However, as is evident from Figure 1 a planar diode is not flat but contains a number of oxide and metal steps. If such a diode is to be encapsulated hermetically the various steps must be filled in by the glass. Experiments clearly indicated that the ability of the glass to fill in steps depends strongly on temperature and to a less pronounced extent on time. Consider for example the results presented in Figure 2; 10 mil thick pyrex 7740 was bonded to chips of silicon each containing a 5000Å oxide step. A fifteen minute bonding cycle was used in each case and bonding conditions were norminally identical. At lower temperatures the bond terminated a distance X

from the step as shown in the figure. The plot shows X as a function of bonding temperature. It will be noticed that the lowest temperature at which X vanishes, that is at which the step fills in, is about $670^{\circ}C$.

The effect of time is far less drastic. Nevertheless, the degree to which the step fills in at a given temperature is markedly larger after an hour than, say, after a few minutes. If the bonding process is permitted to run for several hours at high temperature the glass tends to devitrify. Furthermore, the electrical characteristics of the junction deteriorate substantially when the diodes are held at high temperature for appreciable amounts of time. Thus there exists a practical upper limit to bonding time.

Examination of the bonded glass by interference microscopy showed that the top surface of the glass followed closely the contours of the bottom surface which in turn replicated the step in the silicon surface. Thus, filling in of steps evidently results from the flow of the glass.

After our preliminary work with pyrex 7740 glass, we commenced a search for a glass which could fill in steps below the silicon-aluminum eutectic temperature of $574^{\circ}C$. Experiments confirmed an expected relation between flow temperature and the softening point of the glass, the former being 100-$150^{\circ}C$ lower than the latter. Thus, it became evident

that only glasses with a softening point below 700°C have the desired properties.

Table 1 shows the glasses, most of them commercially available, which were examined in some detail. Five of the glasses either satisfied or came close to satisfying, the viscous requirements. However, three of the glasses had so high a coefficient of thermal expansion that bonds cracked immediately upon cooling. 7052 and 7059 glass were marginal both with regard to viscous properties and thermal expansion. Thus, we were unsuccessful in finding a suitable glass with a softening point below 700°C.

Among glasses with higher softening points at least three glasses were of interest: pyrex 7740, 7070 and 7723. After much experimentation 7070 glass was found to be suitable for our purposes. It matches the silicon very closely thermally, and it has a relatively low alkali content. However, a sealing temperature of 630°C is required in order to fill hermetically the oxide steps of the required height. Hence, it became necessary to develop the high temperature metallization, which is described in the next section.

2. METALLIZATION

I. Selection of Materials.

From the start it was recognized that a successful high temperature metallization must fulfil the following requirements.

a) The metal must form a good ohmic contact with silicon.

b) At the bonding temperature, the metal must not react with silicon in such a way as to damage the electrical properties of junctions.

c) The metal must adhere to the silicon dioxide.

d) The metal must have acceptable sheet resistance.

e) The metal must be suitable for photolithographic processing.

f) The metal must bond to glass.

It is virtually certain that no single metal can satisfy all these requirements. Work has been done on two sandwich structures. In the first we examined a molybdenum chromium sandwich. This structure was a temporary expedient at best in that it had an unacceptably high sheet resistance. Furthermore, it was found that during bonding a flaky oxide formed on the chromium film which made hermetic bonding impossible. Hence, further work on this structure was abandoned.

A metallization which proved far more appropriate for our purposes consisted of a molybdenum aluminum sandwish. A thin molybdenum film was

used to contact the silicon and was overlayed by a thicker aluminum film. The combination was chosen for the following reasons.

1. It was hoped the molybdenum would act as barrier between the aluminum and the silicon and inhibit the formation of a silicon-aluminum alloy.
2. From the work in other labs it appeared that molybdenum makes a low resistance contact to silicon.
3. The aluminum overlay has a high conductivity.
4. The aluminum bonds well to glass.
5. Aluminum melts at 670^{o}C so that the metallization ought to be usable up to that temperature.
6. During photolithographic etching of the metallization pattern, aluminum acts as a mask during the removal of the molybdenum.

Since molybdenum is not easily evaporated, the decision was made to deposit it by low pressure sputtering. The required equipment was designed and built under the contract and is described below.

II. Sputtering Equipment.

Essentially the sputtering equipment is a CVC Plasma Vac mounted on a modified VEC vacuum coater. Jigging was designed and installed which permits sequential deposition of two metals in a single pump-down.

A diagram of the sputtering chamber is shown in Figure 3. A stainless steel ring (1) is inserted between the steel base plate and the pyrex bell jar of the vacuum coater. Mounted on ring (1) are the filament assembly (2), a needle valve and a pressure gauge (not shown). The filament assembly consists of the electron gun (2a) and the water cooled housing (2b). Sputtering gas (normally argon) is passed through the needle valve into the vacuum chamber. The function of the pressure gauge is to turn off power when the pressure exceeds a preset value. A closely-fitting insulated plate (3) of anodized aluminum is placed on the base plate. It prevents material sputtered off the base plate or the copper tubing on the filament housing from reaching the substrate. Mounted on the aluminum plate (3) is the substrate assembly (4) which is described below. The aluminum anode (5) and one target (6) are shown in the diagram but two targets can be accommodated. Anode and targets are supported by steel rods (7) which are shielded by pyrex and quartz tubing (8). The substrate assembly and targets are contained within an 8" pyrex tube (9) which shields the bell jar from sputtered metal. The tube also tends to concentrate the plasma in the region near the targets.

A rotating substrate holder was designed and built. The fixturing for the holder, positioned above the electron gun, is shown in Figure 4.

A sprocket gear is attached to an aluminum rotating ring as shown, and the entire assembly held in place by an aluminum retaining ring which is bolted to the base plate. A quartz sleeve which supports the substrate holder is held on the sprocket gear with an aluminum clamp. A chain is run from the sprocket gear to a smaller gear also attached to the base plate. This entire assembly is driven by a flexible shaft which connects the smaller gear to a rotating seal in the vacuum system. All of the aluminum parts are anodized to minimize sputtering.

The quartz sleeve (2 1/2" I. D. x 2" high) has three quartz rods attached to it. These rods served as supports for the substrate holder as shown in Figure 5.

The molybdenum shields are three inches square while the substrate holder is one and one half inches square and mounted in the center of the one shield. This holder also has a heating element and a thermocouple contained in it so the substrate can be heated if desired. This assembly is held in place with loops of molybdenum wire which are hooked over the quartz rods.

With this type of an assembly the target may be sputtered against the shield until the system is cleaned up. Then the substrate is rotated in

front of the target. More than one target can be used since the assembly may be further rotated to any position. The quartz sleeve not only acts as a support for the substrate holder but also serves to concentrate the plasma in the vicinity of the substrate.

The vacuum system consists of a 6" oil diffusion pump backed by a mechanical pump. A second mechanical pump is used for roughing. A large high vacuum valve permits isolation of the pumping system from the chamber. Between the diffusion pump and the valve is a cold trap. However, the design of the trap is such that any appreciable accumulation of ice restricts the gas flow to such an extent that pumping speed is reduced by a large factor. As a result, the trap should not be cooled down until the chamber has been pumped by the diffusion pump for several hours. This implies that use of the cold trap is both, inconvenient and extremely time consuming, if one wishes to make a reasonably large number of runs per day. Thus, the trap was not normally used during the early deposition work. However, we subsequently discovered that molybdenum etched more easily when it was deposited in a liquid nitrogen protected system. Hence, all later runs were made with a cold trap.

The system is equipped with a thermocouple gauge, mounted just above the high vacuum valve, and with an Alpert gauge just below the valve. If the system is allowed to pump overnight a pressure below 10^{-6} torr can

be obtained even without a cooled-down trap. A pressure of $2 - 5 \times 10^{-6}$ torr, again without cold-trap, is usually obtained after one hour. With a cold-trap the corresponding pressure is below 5×10^{-7} torr.

The system can sputter at fairly high deposition rates. The rates may be further increased by the use of an electro-magnet which tends to constrict and intensify the plasma. However, we could not take advantage of these capabilities for in the absence of target and substrate cooling high sputtering rates raised the target to undesirably high temperatures. Radiation from the target, in turn, generated quite high substrate temperatures.

In the case of aluminum, the deposition rate had to be held below 150Å/min. so that the target would not melt. With molybdenum we ran into adherence problems when the substrate temperature exceeded 200°C. Hence, molybdenum could not be deposited at rates above 100Å/min.

III. Deposition Method and Delineation of Metallization Pattern.

During most of the work the molybdenum and the aluminum were consecutively deposited by diode, low pressure sputtering during a single pump-down. The following procedure was used.

The chamber was pumped down to a pressure of about 5×10^{-6} torr. Then liquid nitrogen was put into the cold trap thereby reducing the pressure to less than 5×10^{-7} torr. Next, with the diffusion pump throttled to a low pumping rate, argon was admitted through a needle valve to a pressure of about 10^{-3} torr.

With an electron current of 3.5 amps a plasma was generated which extended over the whole vacuum chamber but had its highest density inside the guard ring. The discharge was maintained for about 15 minutes to permit stabilization of the system and clean-up of the targets and substrate.

Then the electron current was reduced to 1.5 amp; the target was raised to a potential of 600 volts, and a current of argon ions of approximately 25 ma was extracted from the plasma. Target material was sputtered onto the shield shown in Figure 4 for half an hour in the case of molybdenum and one hour in the case of aluminum. Far longer times were used with freshly prepared targets.

Finally, the substrate was rotated into position and the desired film was deposited. About 1500Å of molybdenum were deposited in 15 minutes,

and 4500Å of aluminum were sputtered in 30 minutes. Terminal substrate temperatures due to radiation were near 200°C. After deposition, the substrate was allowed to cool to 100°C before air was admitted into the chamber in order to minimize oxidation of the film.

The molybdenum films had a shiny, metallic appearance. By contrast, the aluminum films had a rough textrue and were later shown to be quite porous. During the last contract month, therefore, aluminum was evaporated rather than sputtered, furnishing much smoother and denser films.

Film thickness was determined by means of a double beam interferometer to an accuracy of ± 500Å. The sheet resistance of a deposited film was measured by four point probes. The resistivities of the two films were of the order of 30 μ ohm-cm for the molybdenum and 3-6 μ ohm-cm for the aluminum.

The sputtering rate of molybdenum was examined in some detail. Using a sputtering potential of 600V, sputtering rates were generally of the order of 120Å per minute for ion currents of .5 milliamps/cm^2. Assuming the films to have bulk density it may be estimated that roughly .7 x 10^{17} atoms/cm^2/min were sputtered by 2 x 10^{17} ions/cm^2/min for an average yield of .3 atoms per ion. This is smaller than Wehner's[1] published yield data by a factor of about 3. The discrepancy is explained by the fact that

1 G. K. Wehner: Phys. Rev. 112 1120 (1958)

the substrate does not collect all the sputtered material because of the system geometry. Corrections should also be made for sputtering of the target leads and for a sticking coefficient that is less than unity. The dependence of the normalized sputtering rate on sputtering voltage is shown in Figure 6. Each point represents an average over several runs. The dependence is somewhat weaker than Wehner's results suggest. From an analysis of our runs it appears that with proper control the sputtering rate can be controlled to within 5 percent which was more than adequate for our purposes.

Patterns were etched into the molybdenum-aluminum film by photolithographic techniques. The aluminum was etched in a solution containing one part of 50 percent sodium hydroxide and 2 parts alcohol. The molybdenum etch contained one part nitric acid, one part sulfuric acid and 3 parts water. The molybdenum etch attacks the aluminum very slowly so that the latter acts in effect as mask.

Usually the etching proceeded in a straightforward fashion. However, during the last weeks of the sixth contract month the molybdenum was found to etch in some cases far more slowly than usual, and in other cases it did not etch at all. Lack of etchability was traced to a leak in the gas handling system. Further improvements in the etchability of molybdenum were obtained when the liquid nitrogen trap was used.

During the early sputtering work the adherence of molybdenum to the substrate presented some problems. Satisfactory adherence could be obtained if the sputtering rate was kept below 150Å per minute and if film thickness was limited to less than 3000Å.

IV. Electrical Characteristics of the Metallization.

The metallization consisting of about 1500Å of molybdenum and 4500Å of aluminum had a sheet resistance of the order of .1 ohms per square as deposited. For the geometry shown in Figure 1 this corresponds to a line resistance of about .15 ohms.

Experiments were made to determine what changes in line resistance resulted from heat treatments at the sealing temperature of 630°C for various amounts of time. In other trials efforts were made to reproduce bonding conditions as closely as possible. As shown in Table 2 substantial changes were produced by extended heat treatments. However, for heating cycles or simulated bonding operations of less than 10 minutes duration, the line resistance generally changed by less than 25 percent. Since our usual bonding cycle lasts only three minutes, no substantial changes in line resistance are therefore to be expected.

For a further investigation of resistance changes during bonding the test vehicle shown in Figure 7 was utilized. It consists of an oxidized silicon chip with three sputtered molybdenum aluminum lines A, B, and C. Oxide thickness, line thickness and line width all corresponded to those we were using on the diodes. To the silicon chip was bonded a glass slice with one aluminum line D such that D overlaps the lines A, B and C. Every effort was made to duplicate the conditions that are found in the encapsulation of the diodes. The resistance of the four lines was measured before bonding,

after bonding at 550°C, and after a second bonding operation at 630°C, the latter being the bonding temperature for the diodes.

The bonded test vehicle was approximated by the equivalent circuit shown in Figure 8. Though this is only a rough approximation for a far more complex situation, it was hoped that it would show up gross resistance changes during bonding. In addition it was expected that the test vehicle would give information about the contact resistances between the lines A, B, and C on the silicon chip and the line D on the glass sheet. A similar contact resistance, it should be noted, is found in the encapsulation geometry of Figure 1 between the metal pad on the silicon dioxide and the matching metallization on the glass cover.

As it turned out the most significant result derived from experiments with the test vehicle was the observation that after bonding all lines were shorted to the silicon. On the other hand, when glass without metallization was bonded to the metallized silicon chip under similar conditions no shorting was observed. The implication is that the metal line D on the glass shorts to the silicon edges of the chip. This occurs because of chipping of the silicon oxide during scribing. As a result of the shorts it was not possible to determine the magnitude of line resistance changes or of the contact resistances with any certainty. However, it is believed that the contact resistances were negligibly small as long as the sheet resitances of the various lines did not change appreciably.

Similar results were obtained when diodes were metallized and assembled according to the geometry of Figure 1. Diodes with initially low reverse leakage were found to be partially shorted after bonding. Furthermore, from their forward characteristics it was deduced that after bonding the diodes had series resistances in the range of 10 to 50 ohms. The large resistances are attributable primarily to the alloying of the shorted aluminum lines with the silicon. These problems necessitated certain changes in geometry which are described in the next section.

The electrical characteristics of the molybdenum silicon contact were evaluated in the following manner. A slice of diodes, each having the geometry of Figure 1, was metallized on the back side with electroless nickel, sintered at 750^{o}C in argon for a period of 10 minutes. The slice was then cut into sections and 13 mil dots respectively of aluminum and of molybdenum overlayed with chromium were deposited through a metal mask on the sections. The aluminum was evaporated by a procedure used for integrated silicon circuits. The molybdenum-chromium was sputtered. The forward characteristics of the contacts were evaluated by clamping each section to a copper block and contacting the metal dots with a probe. Forward currents were measured at 1 and 2 volts. Results are shown below.

Si - Al		Si - Mo - Cr	
1V	2V	1V	2V
160 ma	850 ma	250 ma	1100 ma
100	850	300	1100
60	750	240	1100
120	950	300	1200
180	1000	300	1200
300	1400		

Although this procedure of evaluating forward characteristics is, of course, not very accurate in that appreciable voltage drops may occur at the probe to metal contact and also at the nickel to copper contact, it would appear from the results that the molybdenum silicon contact is not inferior to the aluminum silicon contact. Presumably similar results would have been obtained had the molybdenum been overlayed with aluminum rather than chromium.

3. GEOMETRICAL MODIFICATIONS

Two schemes were proposed to prevent the aluminum line on the glass from contacting the silicon at the edges of the dice where the oxide had been chipped by scribing. One proposed solution of the problem was to cover the aluminum lines with an evaporated layer of silicon monoxide which would presumably act as a barrier between the aluminum and the silicon. In a second method it was proposed to bevel the dice as illustrated in Figure 9. In this method a network of grooves would be etched into the silicon prior to processing. The silicon would then be processed in a conventional manner and finally diced in the centers of the grooves. As a result the chips would have the bevelled appearance of Figure 9. It was hoped that any damage to the oxide would be confined to the bottom of the groove where it cannot be contacted by the aluminum lines on the glass.

In pursuance of this program work was done on the photolithographic etching of silicon. It soon was found that neither KTFR nor KMR will mask sufficiently long to permit removal of a significant amount of silicon with the usual nitric acid hydrofluoric etches. It was, therefore, decided to use a metal mask in place of the photoresist mask. After some trials, chromium was found to be practically inert to a 10:1 nitric acid hydrofluoric acid etch. The etching of chromium by photolithographic techniques presented some difficulties. An etch with concentrated HCl at about $80^{\circ}C$ was partially

successful. However, the etching time is only of the order of seconds and very critical if the integrity of the photoresist is to be preserved. More promising results have been obtained with a milder etch which was obtained from Electronic Films, Incorporated. The principal remaining difficulty was to deposit pinhole free chromium films.

At the suggestion of the contractor in order to save time it was decided not to work on this problem any further. Instead, the geometry was changed to the one shown in Figure 10. In this configuration the glass is not metallized so that there is no possibility of shorting devices during bonding. The new geometry also eliminates the metallization overlap which, though feasible, would have required more work to make reproducible low resistance contacts.

4. HERMETICITY

With glass type, bonding temperature and metallization all firmly established a good deal of time was spent on trying to make the package hermetic. As reported in Section I oxide steps of the required height could be hermetically filled in with 7070 glass at 630°C over a period of 2-3 minutes. However, it became evident at this point that the same was not true for metal steps. In particular the metal steps on the silicon dioxide failed to fill in as judged by visual observation and there was uncertainty about the hermeticity of the metallization steps on the bare silicon windows.

In order to investigate this problem more carefully, visual observation at 100X was augmented by observation at 500X. In addition the following leak detection procedure was adopted. Test specimens as illustrated in Figure 11 were fabricated. They consisted of stepped structures to which glass plates were bonded into which small holes had been drilled. The holes straddled the steps such that any leakage along the step would terminate in the hole. A bonded assembly was then mounted by means of an O-ring on a Veeco helium leak detector MS-9 such that the hole in the glass faced the vacuum of the detector. Leak testing was done by spraying helium from a fine nozzle at the bonded assembbly.

The smallest detectable leak was found to be 4×10^{-10} std. cc of He/sec. However, frequently the O-ring seal produced leakage of the

order of 2×10^{-9} std. cc of He/sec. Therefore, only those assemblies were designated as leakers which indicated leaks in excess of this number.

Using these procedures a variety of metal, oxide and composite steps were evaluated. It was found that only oxide steps and silicon steps could be hermetically encapsulated. All steps formed by sputtered aluminum films were found to leak to some degree. Eventually the leakage was traced to the fact that these films leaked laterally due to insufficient density. Evaporated aluminum films performed substantially better in this respect. For lack of time, no further work on this problem was possible under the contract.

5. ELECTRICAL CHARACTERISTICS OF DIODES

I. Forward Characteristics.

The forward characteristic of a diode is determined by the resistance of the metal lines and by any contact resistance that may exist at the two metal to silicon contacts. As reported in Section II the molybdenum-silicon contact appears to be comparable to the conventional aluminum-silicon contact. As might be expected the electrical contact to the backside of the diodes is quite as important as the front contact even though it constitutes a large area contact. Best results were obtained by alloying the chip by means of an antimony doped gold preform to a gold plated TO type header.

Typical forward characteristics are presented in Figure 12. The measurements were made by placing a current and a voltage probe on the metal pad on the silicon oxide and by placing a third probe on the header. From the slopes of the curves it may be estimated that series resistances in the range .5 to 2 ohms are present. As mentioned in Section II the minimum resistance of the metal lines after bonding is of the order of .2 ohms. Thus, an unaccounted .3 ohms resistance is present even in the best measured forward characteristics.

The estimate of series resistance was made on the assumption that at 100 milliamps a diode operates under conditions of heavy injection

level. Under these conditions the current increases as exp $9(V - IR)$ $2KT$ where V is the applied voltage, I represents the forward current and R is the series resistance. The slope of the V versus I plot is given by $\frac{dV}{dI} = R + \frac{2KT}{9I}$.

II. Reverse Characteristics.

1. Effect of Metallization.

As a first step the dielectric strength of the planar oxide as grown in our furnaces was examined. Metallization patterns were deposited on oxidized silicon slices which had not been further processed. The oxide thickness on these slices was the same as on our diodes; namely, 1 micron. Dielectric breakdown of the oxide was determined by probe measurements using a curve tracer as the power supply Results of these measurements are shown in Table 3. It will be noticed that in the majority of cases breakdown occurred above 350 volts. A breakdown below 100 volts was found only near the edge of the slice. Therefore, our oxide had in general a dielectric strength in excess of 3×10^6 volts/cm which is in reasonable agreement with published values.

In our earliest work initially good junction characteristics deteriorated substantially upon metallization with molybdenum-aluminum. Partial shorts and low breakdown voltages were attributed to pinholes in the oxide which had evidently resulted from faulty KPR work. When diodes with relatively pinhole free oxide were metallized no deterioration in junction characteristics were observed. This is documented in Table 4 which shows reverse characteristics before and after metallization.

2. Effect of Bonding.

The effect of bonding on the reverse leakage was in general fairly reproducible for diodes coming from a particular slice. However, reproducibility from slice to slice was poor. In some cases bonding produced substantial deterioration in the reverse leakage. Frequently heat treatments subsequent to bonding improved the leakage by a large amount. For several slices the following results are typical.

	I/60V	I/80V	I/120V	BV
	na	na	na	volts
Before bonding	12	15	21	160
After bonding	22	32	100	150
After heat treatment	7	11	40	140

This diode was as usual bonded in room air at a temperature of 630°C for about 3 minutes. Subsequent to bonding they were heat treated at 630°C for 15 minutes. In a comparison of the final and initial reverse characteristics, a slight reduction of breakdown voltage, somewhat lower leakage at low voltage, and a higher leakage at high voltages were often observed. Similar results were obtained also with non-metallized diodes. In order to investigate whether the change in the reverse characteristic was associated with the temperature at which bonding was performed a few diodes were exposed to the equivalent temperature cycle without glass being bonded to them. On the "best" diode the following results were obtained.

	I/20V	I/40V	I/60V	I/80V	I/100V	I/120V
				na		
Initial	9	13	20	40	110	360
First heating cycle	11	19	27	40	56	86
Second " "	8	12	16	22	32	46
Third " "	6	11	20	50	180	500

The first two heating cycles consisted of 5 minutes each at 630°C. During the third cycle the diode was exposed to the same temperature for 15 minutes. The above data show that heat treatments by themselves can produce substantial changes in the electrical characteristics. However, it should be noted that serious deterioration was observed only after a total accumulated time of 25 minutes. Thus, it is probable that the changes during the bonding cannot be attributed to the heating cycle.

Bonding had a similar effect on diodes with breakdown voltages of about 95 volts which originated from a different slice (See Figure 13). However, a heat treatment of 30 minutes duration at 550°C reduced the leakage not only at low voltages but over the whole voltage range. No reduction of breakdown voltage was observed. We believe the different behavior subsequent to heat treatment cannot be attributed to a less severe heat treatment or to the fact that the breakdown voltage was lower in this case.

Relaxation phenomena subsequent to bonding were frequently observed.

First measurements after bonding are usually made as soon as the diode reaches room temperature. At this time the diode is usually leaky and has a low, soft breakdown. The characteristic steadily improves with time and the rate of change slows down very substantially after a period of 15-20 minutes. Further improvements are often observed during the subsequent 24 hours.

A number of cleanup treatments prior to encapsulation were tried out. In particular we experimented with boiling the parts in a succession of solvents and distilled water. In other cases we gave the parts slight etches. Sometimes the cleanup treatments were followed by air bakes. None of these measures appeared to have much effect on the reverse leakage subsequent to bonding.

Figure 14 shows the best reverse characteristics to date of encapsulated devices. These diodes came from an unusually good slice. Cleaning prior to encapsulation was limited to the removal of dust. The diodes were not heat treated subsequent to bonding. A comparison of leakage before and after bonding shows only very slight changes in characteristics. Thus, it is clear that our bonding process is capable of producing diodes with excellent electrical characteristics. However, more work is clearly required in order to gain a better understanding as to the effect of bonding on the reverse characteristics.

6. PHOSPHOROUS DIFFUSED DIODES

The work reported in the preceding sections was done on p- on n- diodes which were fabricated by the diffusion of boron into n- type silicon. Very preliminary measurements were made during the last weeks of the contract on n- on p- diodes made by the diffusion of phosphorous into p- silicon. The diodes were made according to the geometry of Figure 10. Oxide thickness and diffusion schedules were the same as on the p- on n- diodes. The resistivity of the p- type starting material was selected so that the diodes broke down around 100 volts.

As expected, these diodes, as made, had n- channels which presumably extended over the whole surface. The following was evidence for the presence of channels.

1. During measurements of the reverse characteristics on one diode a floating voltage appeared on the second diode.
2. Unusually large values of junction capacitance were measured.
3. With the two junctions in parallel, the capacitance was much less than the sum of the individual junction capacitances. Indeed in some cases the same capacitance value was measured for each individual junction as well as for the two junctions in parallel.

4. The leakage currents on n- on p- diodes were invariably orders of magnitude higher than the leakage currents on p- on n- diodes.
5. The dependence of current on applied voltage was much weaker than junction theory predicts.

The observations 4 and 5 suggest that the channels extended over the whole surface so that most of the current was generated on the edges of a chip which were not only unprotected by planar oxide but also mechanically perturbed by the scribing and dicing operations.

Some diodes were bonded and subsequently heat treated. Other diodes were first heat treated and then bonded. No consistent trends could be deduced from our very limited work. The reverse characteristics for the two "best" diodes are shown in Figure 15. It should be noted that the leakage currents are in the micro amp range as compared to reverse currents in the low nano amp range for good p- on n- diodes. The reverse characteristics prior to bonding are typical for their weak voltage dependence. Bonding to 7070 glass at 630^{o}C for a period of 3 minutes generally increased the voltage dependence and subsequent heat-treatments did not lead to any substantial changes in reverse leakage. From present results it appears that n- on p- diodes with reasonable reverse characteristics are feasible only if a p^{+} - guardring is placed around the junctions so that channels will terminate at the ring rather than run out to the edge of a chip.

Attempts were made to measure the conductance of the channel between the two junctions but measurements to date have been highly suspect because of large junction leakage and difficulties in making good ohmic contact to the high resistivity p- type back surface. Probably the most reliable measurements were made on an encapsulated device and are shown in Figure 16. At a bias of one volt the channel has a conductance of .66 micromhos and the corresponding channel conductance per square is .26 micromhos. The channel conductance decreases rapidly with bias as would be expected.

The channel measurements were made by means of the circuit shown in Figure 17 which is similar to circuits used by Brown[1] and Statz et al[2]. A 1 kc signal of .1 volts peak to peak was applied across the channel and the resulting current was derived from the voltage measured across a standard resistance of 1000 ohms by a Hewlett Packard wave analyzer, model 310A.

It would of course have been highly desirable to perform channel conductance measurements on chips before bonding, after heat treatment, and after bonding but not enough time was available. Such studies are being planned since they are expected to give valuable information about the effect of bonding on the semiconductor surface.

1 W. L. Brown: Phys. Rev. 91 518 (1953).

2 Statz, de Mars, Davis and Adams: Phys. Rev. 101 1272 (1956).

7. RECOMMENDATIONS

In an evaluation of the potentialities of the encapsulation concept of this contract, the greatest remaining question is whether the process will ultimately be capable of furnishing 100 percent hermeticity. This question can only be resolved by further experimentation.

The molybdenum aluminum metallization developed under the contract proved serviceable for the purposes of a feasibility study but requires further improvements along the following lines.

1. During bonding some aluminum tends to migrate off the molybdenum underlay and alloy with the silicon. A less severe problem is alloying at pinholes in the molybdenum film. Though formation of small amounts of aluminum-silicon alloy was of no consequence in this work it could produce shorts in shallow transistor structures.
2. Means have to be found of depositing films of sufficient density so that lateral leakage of air through the films is inhibited.
3. It is not yet known whether an acceptable molybdenum-silicon contact to lightly doped silicon such as the base region of a transistor is feasible.

In section 3 we discussed a tendency of the aluminum metallization on the glass cover to short against the edge of the silicon chip. It is

believed that this problem is capable of a relatively simple solution along the lines suggested in the section.

Though feasibility appears to have been established for the low resistance contact between the metal pad on the silicon oxide and the matching metallization on the glass cover there is a need for further substantiation. Additional work is also required to improve reproducibility and to check out the reliability of the contact under life tests and environmental tests.

A study of the effect of bonding on the semiconductor surface ought to be undertaken. At least in part, the methods of section 6 could be utilized.

We regard the electrical performance of our best bonded diodes as highly encouraging. However, work is obviously required in order to improve the reproducibility and to investigate the stability under environmental and life tests.

TABLE 1

		Coefficient of thermal expansion in/in/^{o}C	Softening point
1720	Alumino Silicate	42×10^{-7}	915^{o}C
0080	Soda Lime	92	696
0120	Potash-Soda-Lead	89	630
1710	Hard Lime	42	915
7052	Borosilicate (Kovar)	46	708
7070	Borosilicate	32	746
7720	Borosilicate (Nonex)	36	755
9741	UV glass	39	705
0211	Micro Sheet	72	720
7740	Pyrex	32	820
8030	Lead	89	614
7059	Lead-Alkali free	47	842
7723	Alkali free	30-40	
	Silicon	32	

TABLE 2. RESISTANCE CHANGES IN Al LINE ON #7070 DURING TEMPERATURE CYCLING WITH AND WITHOUT VOLTAGE.

#	Temperature °C	Time min.	Resistance ohms
1		initial	3.2
	630[1]	10	3.2
	630[2]	10	4.0
	630[2]	10	17.0
2		initial	2.4
	630[1]	10	2.4
	630[1]	10	2.6
	630[1]	10	2.7
3		initial	2.3
	630[1]	10	2.2
	630[2]	10	2.8
	630[2]	10	8.1
	630[1]	10	8.1
4		initial	3.2
	630[1]	10	3.2
	630[2]	10	3.5
	630[2]	10	4.4

1 Heat treatment only.

2 Simulated bonding procedure.

TABLE 3. BREAKDOWN VOLTAGES OF VARIOUSLY METALLIZED PLANAR OXIDE.

Slice 11-14-66-1, Mo-Al metallization
400, 330, > 400, 360, 380, > 400, > 400, 300, > 400, 400, 100, 360

Slice 11-15-66-1, Al metallization
350, 350, 370, 300, 300, 250, 300, 300, 300, 250, 350

Slice 10-19-66-1, Al metallization
60, 380, 75, 400, 50, 400, 350, > 400, > 400, 350, > 400, > 400

Slice 09-30-66-1, Cr metallization
300, 400, 400

TABLE 4. REVERSE CHARACTERISTIC BEFORE AND AFTER METALLIZATION.

Before Metallization			After Metallization		
I/80V	I/120V	BV	I/80V	I/120V	BV
na	na	volts	na	na	volts
27	34	150	12	14	165
28	39	150	12	15	160
28	35	150	48	110	160
25	60	130	210	-	100
24	28	160	14	17	170
22	28	150	-	-	60
20	26	100	-	-	70
25	33	150	13	18	160
14	21	150	-	-	20
16	22	150	16	22	160

TABLE OF FIGURES

1. Encapsulation geometry.
2. Bonding of oxide step.
3. Vacuum chamber.
4. Substrate assembly.
5. Substrate holder.
6. Normalized sputtering rate versus voltage for molybdenum.
7. Test vehicle for determination of resistance changes during bonding.
8. Equivalent circuit used for test vehicle of Figure 7.
9. Bevelled dice geometry.
10. Modified encapsulation geometry.
11. Test specimen for hermeticity test.
12. Current-Voltage plots of forward-biased diodes.
13. Reverse characteristics of p- on n- diodes, Early Results.
14. Reverse characteristics of p- on n- diodes, Final Results.
15. Reverse characteristics of n- on p- diodes.
16. Channel conductance versus bias.
17. Circuit for channel conductance measurements.

Figure 2. Bonding of Oxide Step

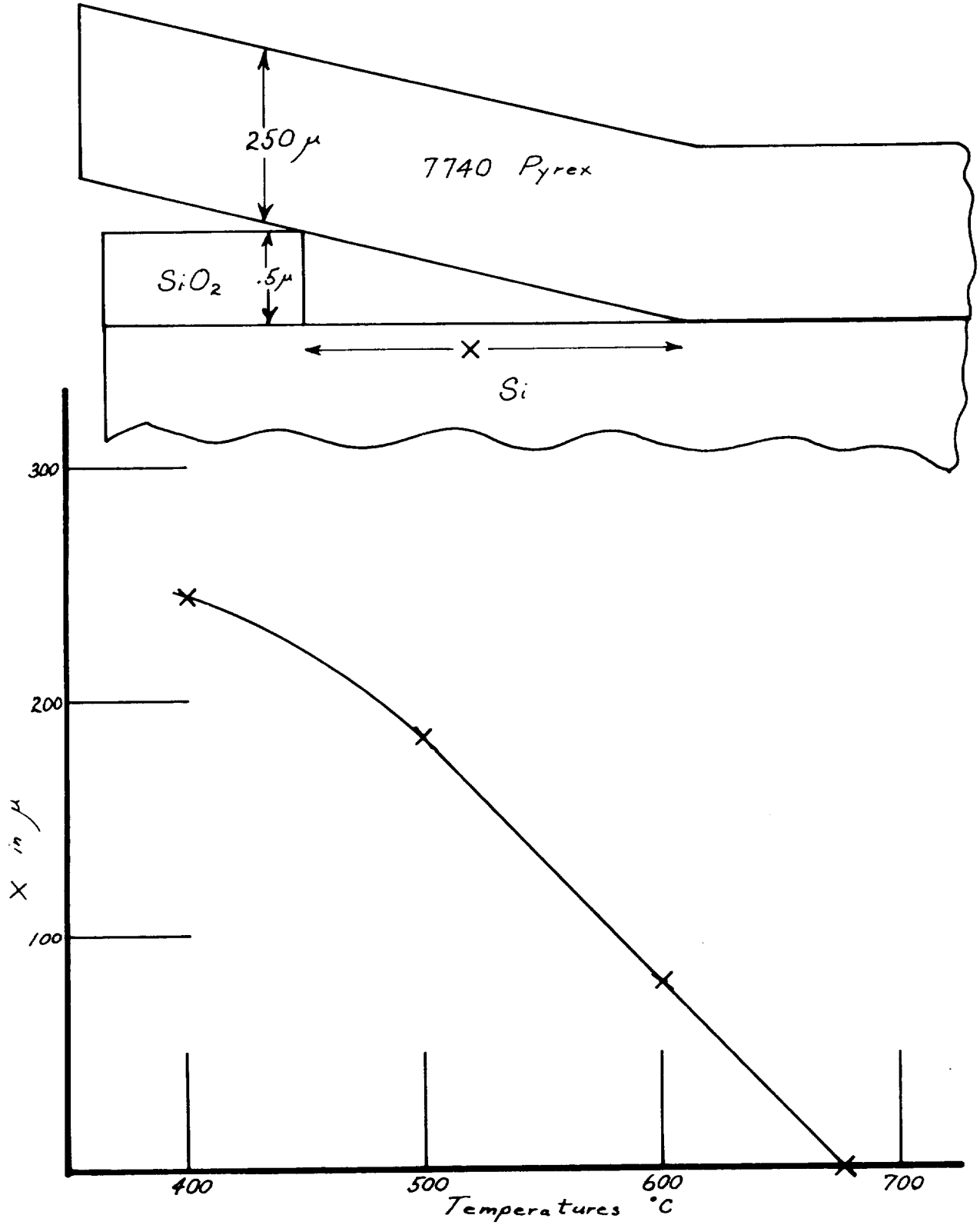

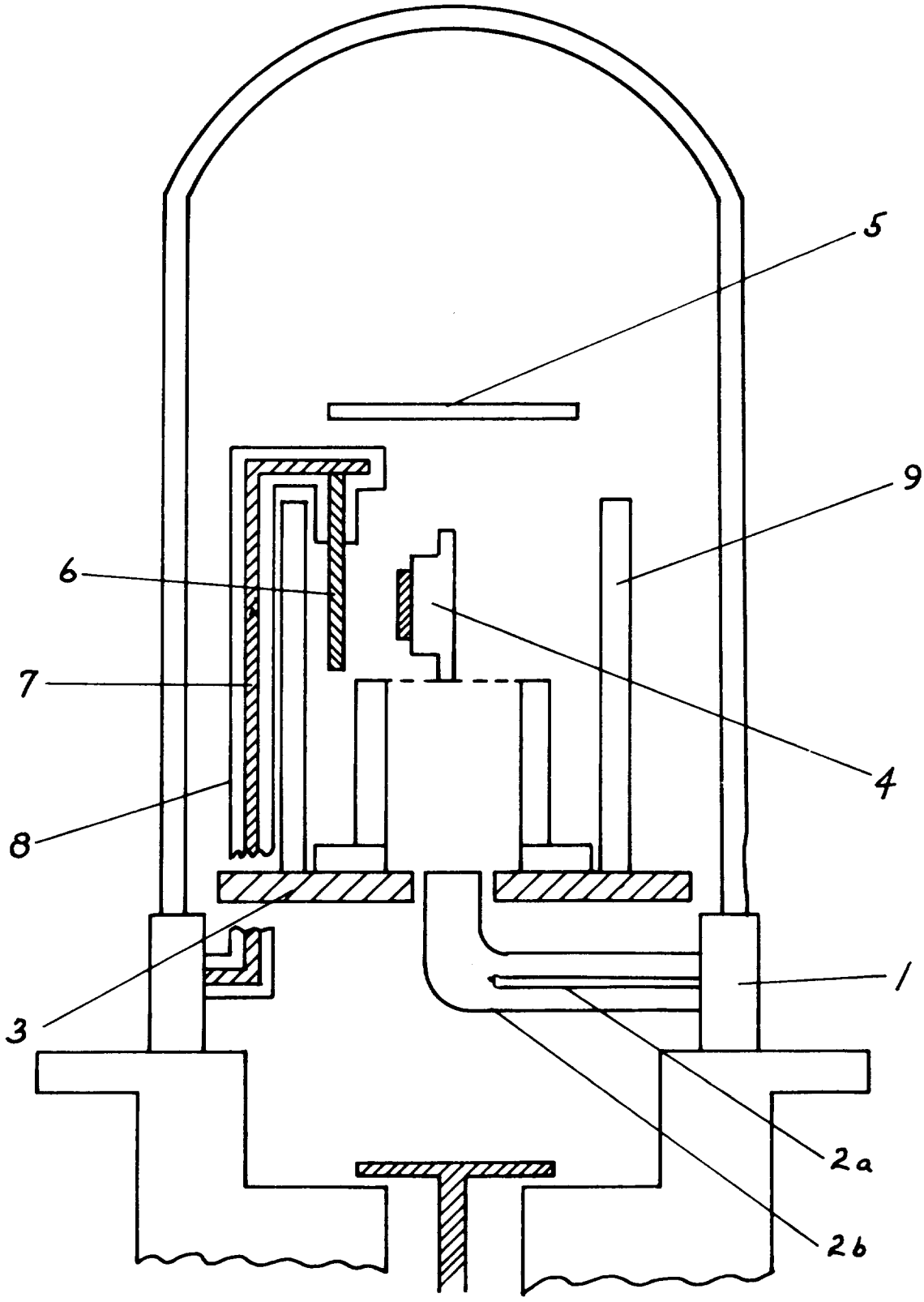

Figure 3. Vacuum Chamber

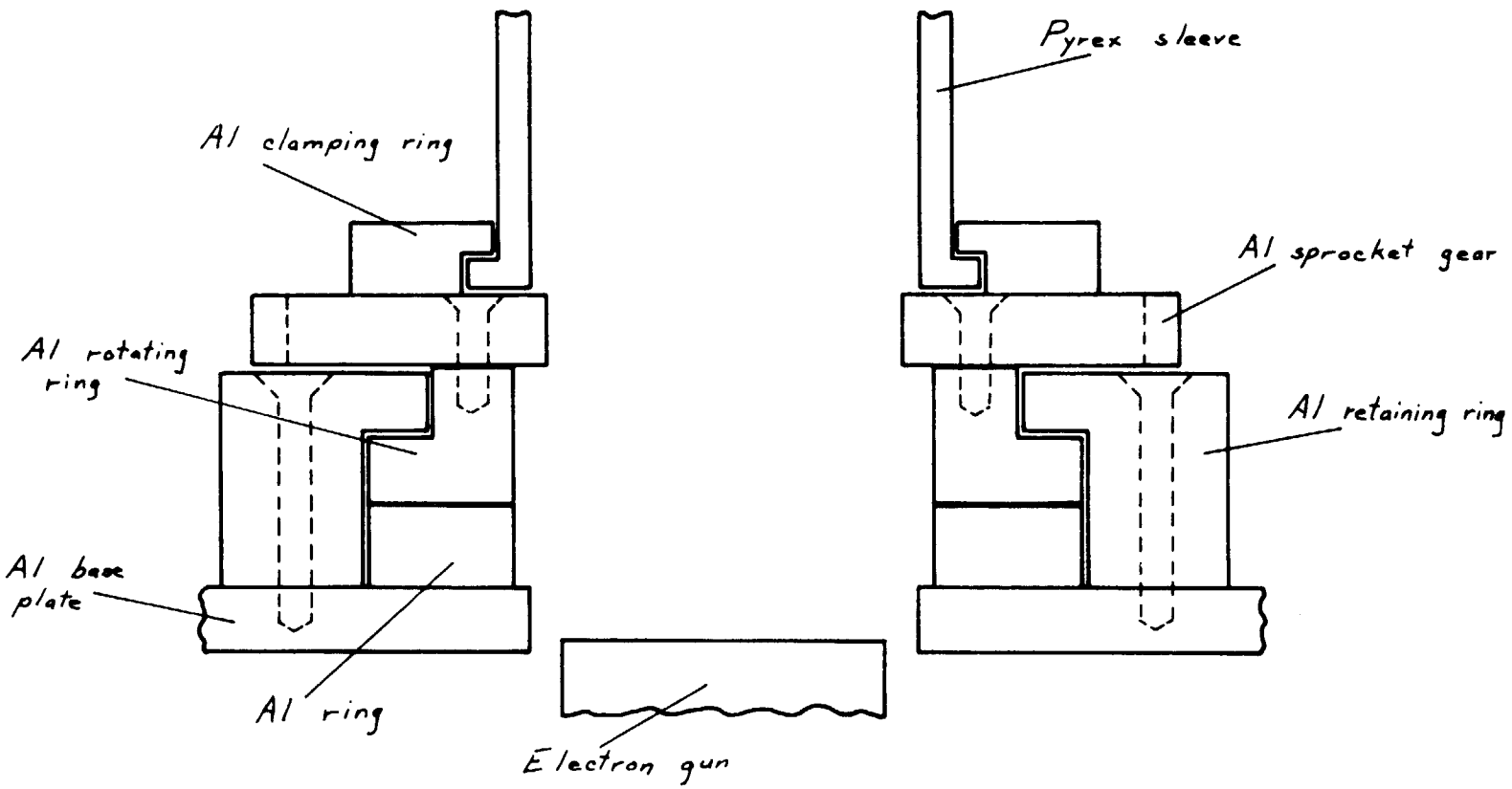

Figure 4. Substrate Assembly

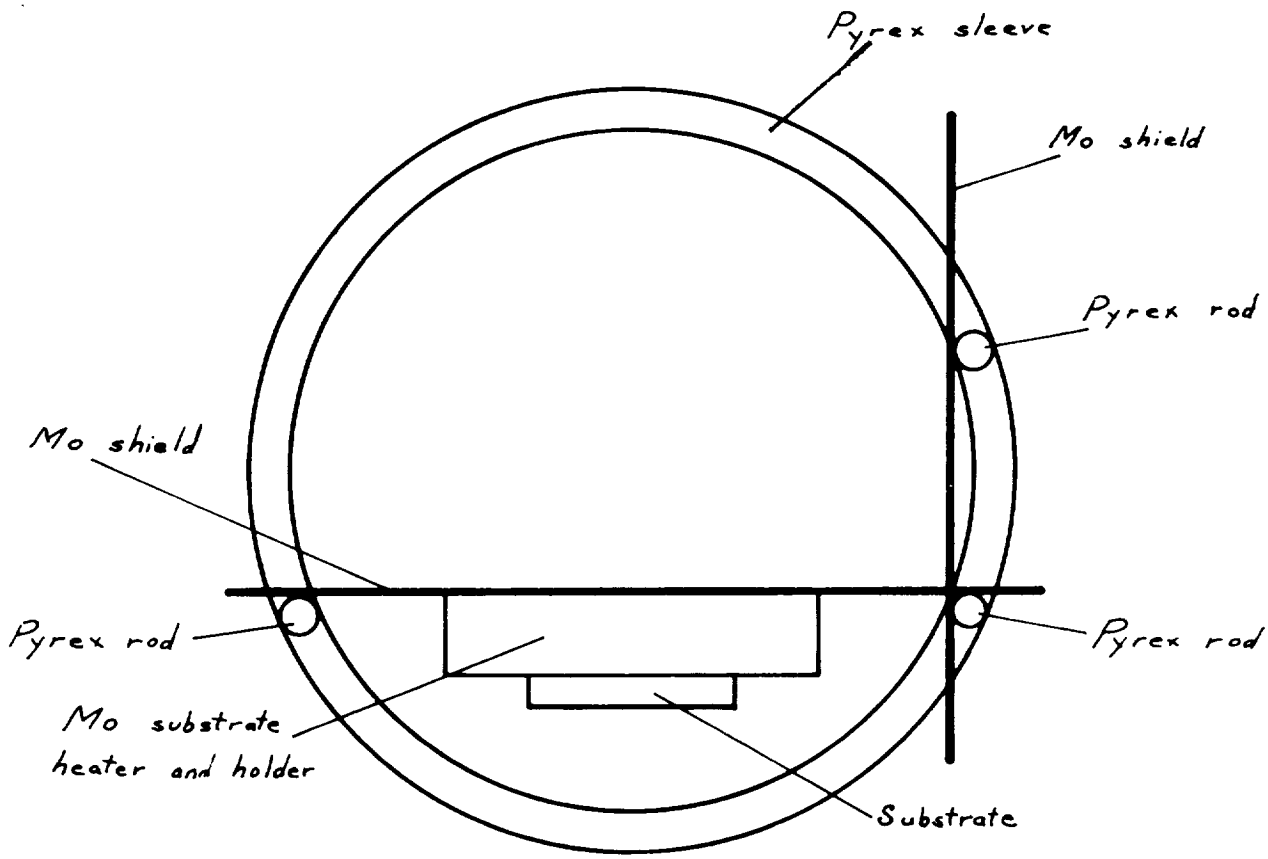

Figure 5. Substrate Holder

Figure 6. Normalized Sputtering rate vs Voltage for Molybdenum

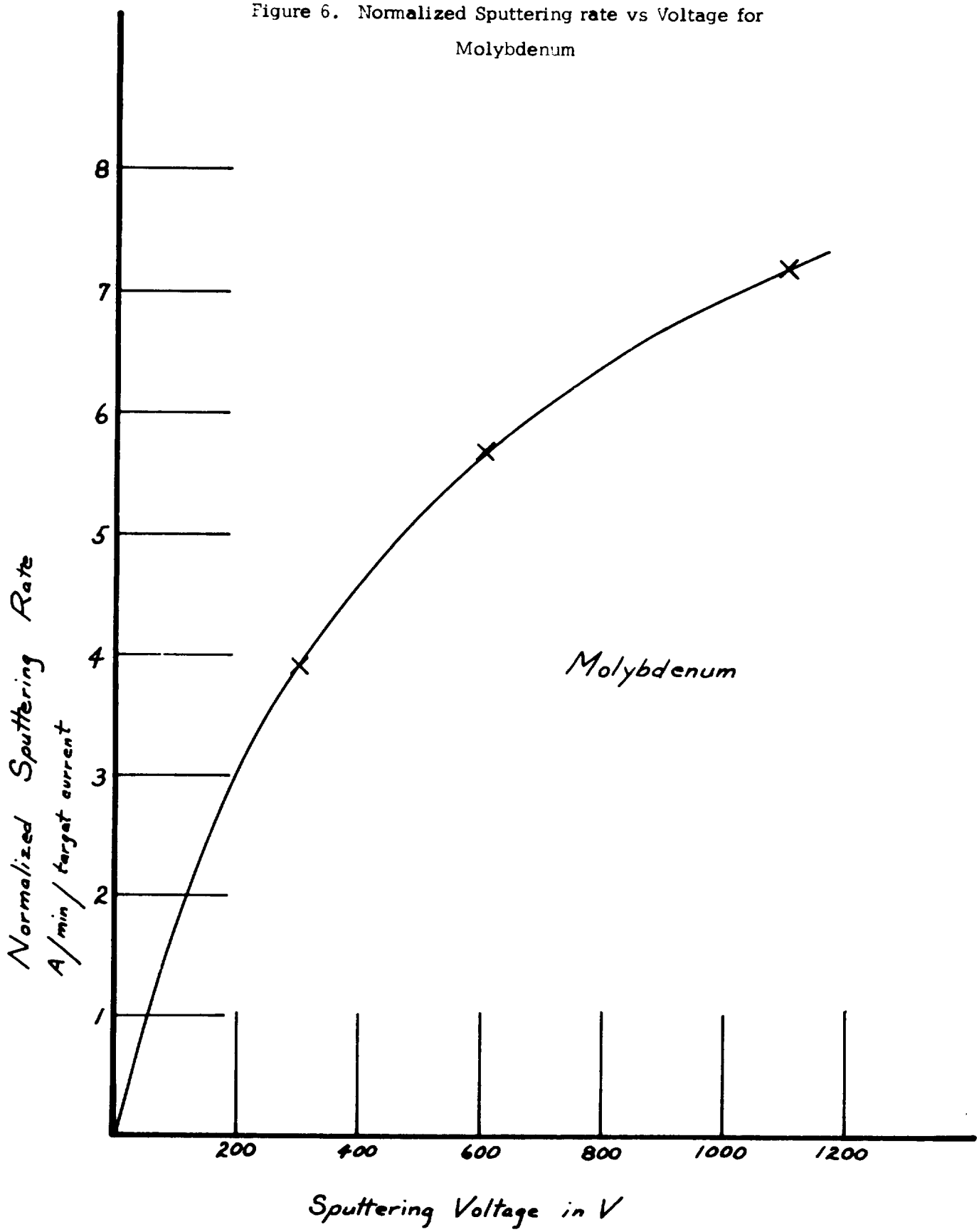

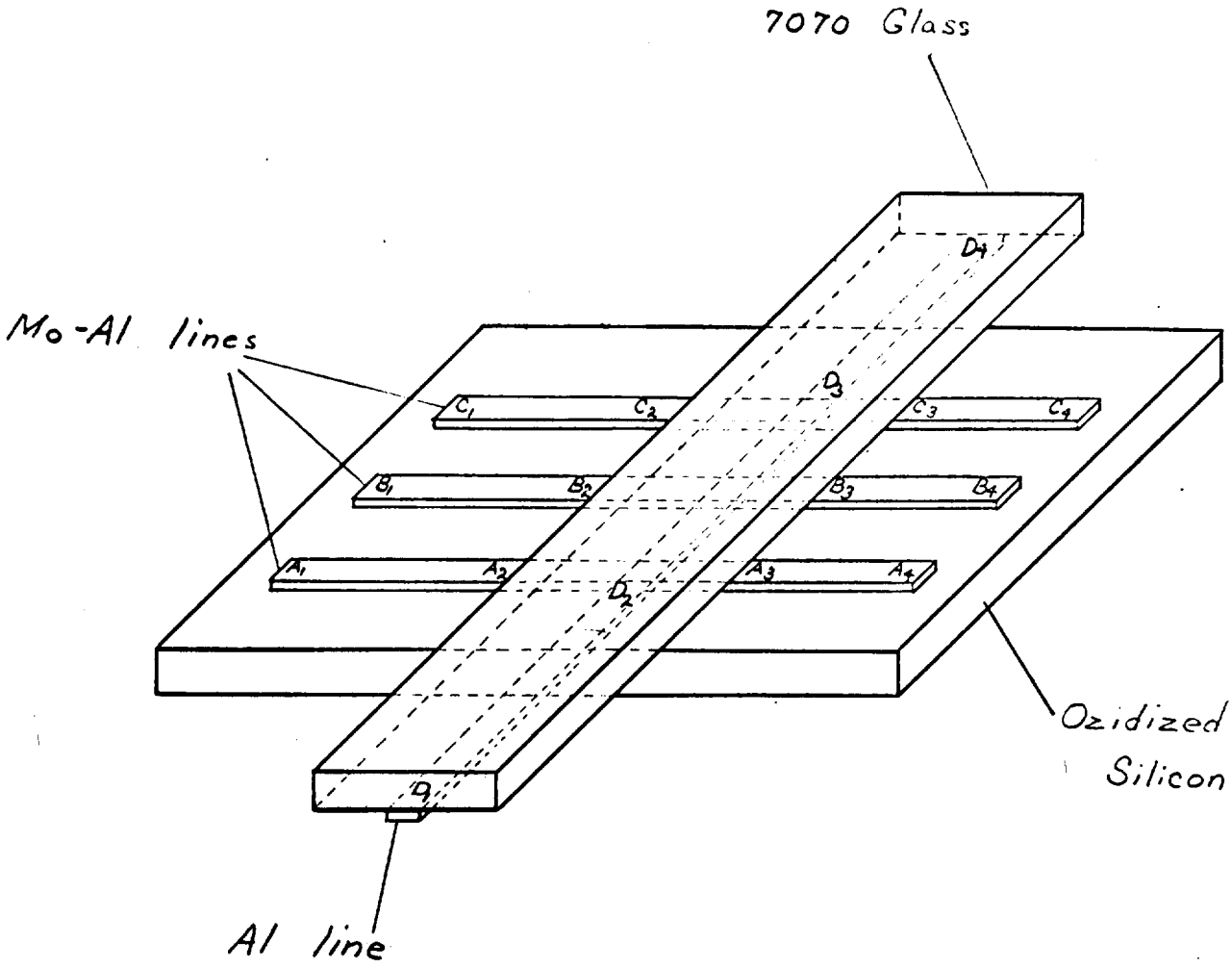

Figure 7. Test vehicle for determination of resistance changes during bonding.

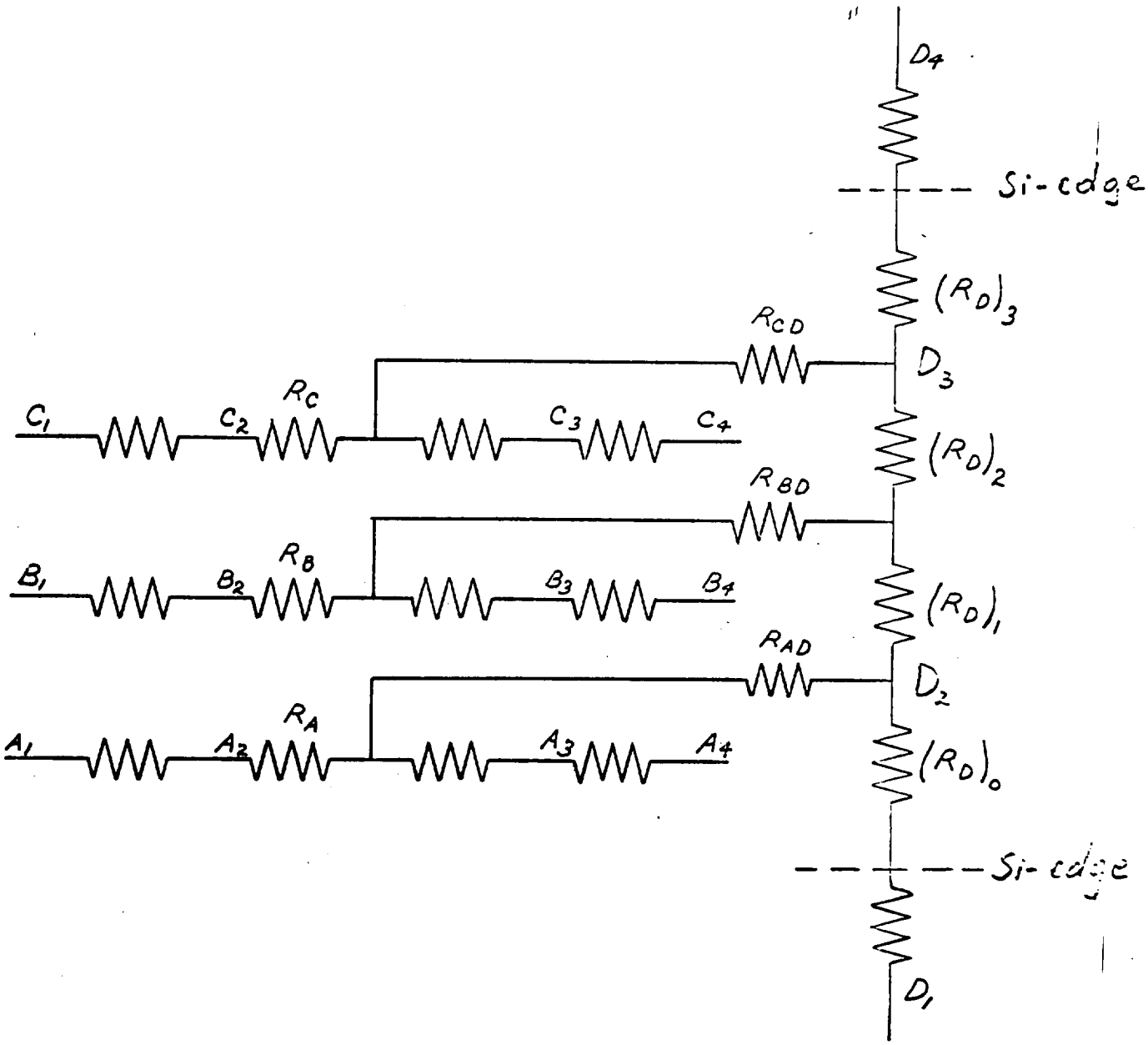

Figure 8. Equivalent circuit used for test vehicle of Figure 7.

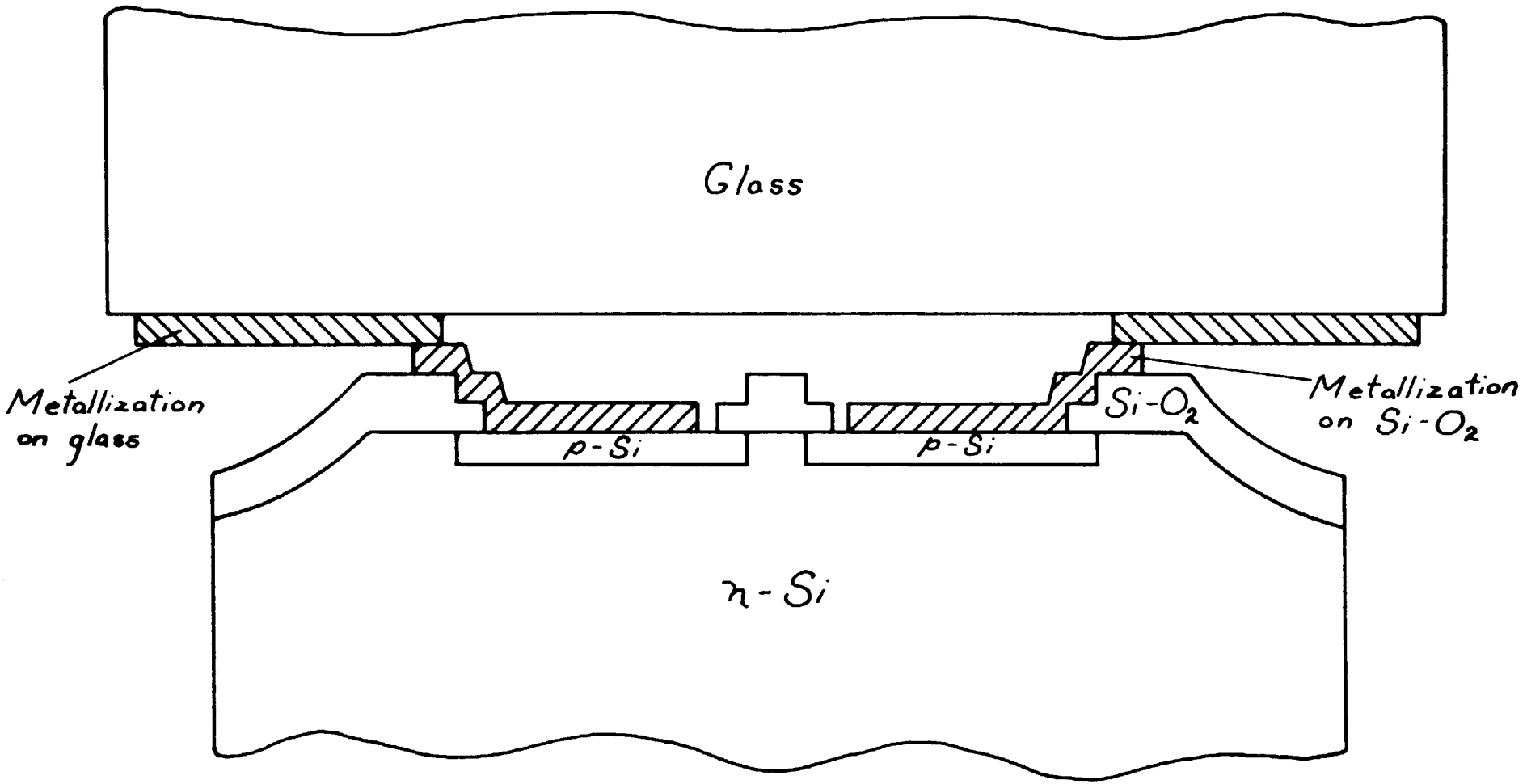

Figure 9. Bevelled Dice Geometry.

Figure 12. Current-Voltage Plots of Forward-Biased Diodes.

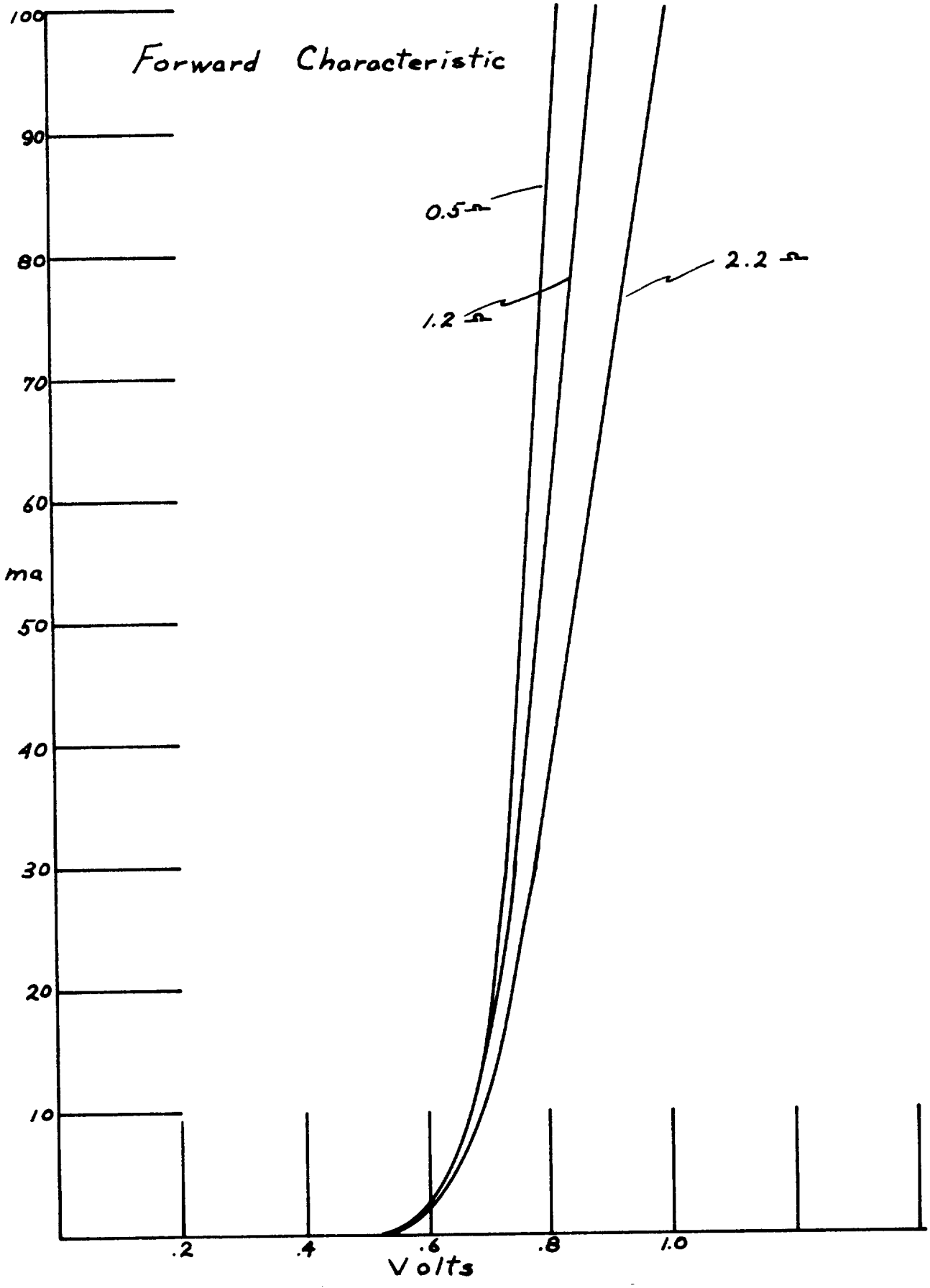

Figure 13. Reverse Characteristic of p- on n- Diode, Early Results.

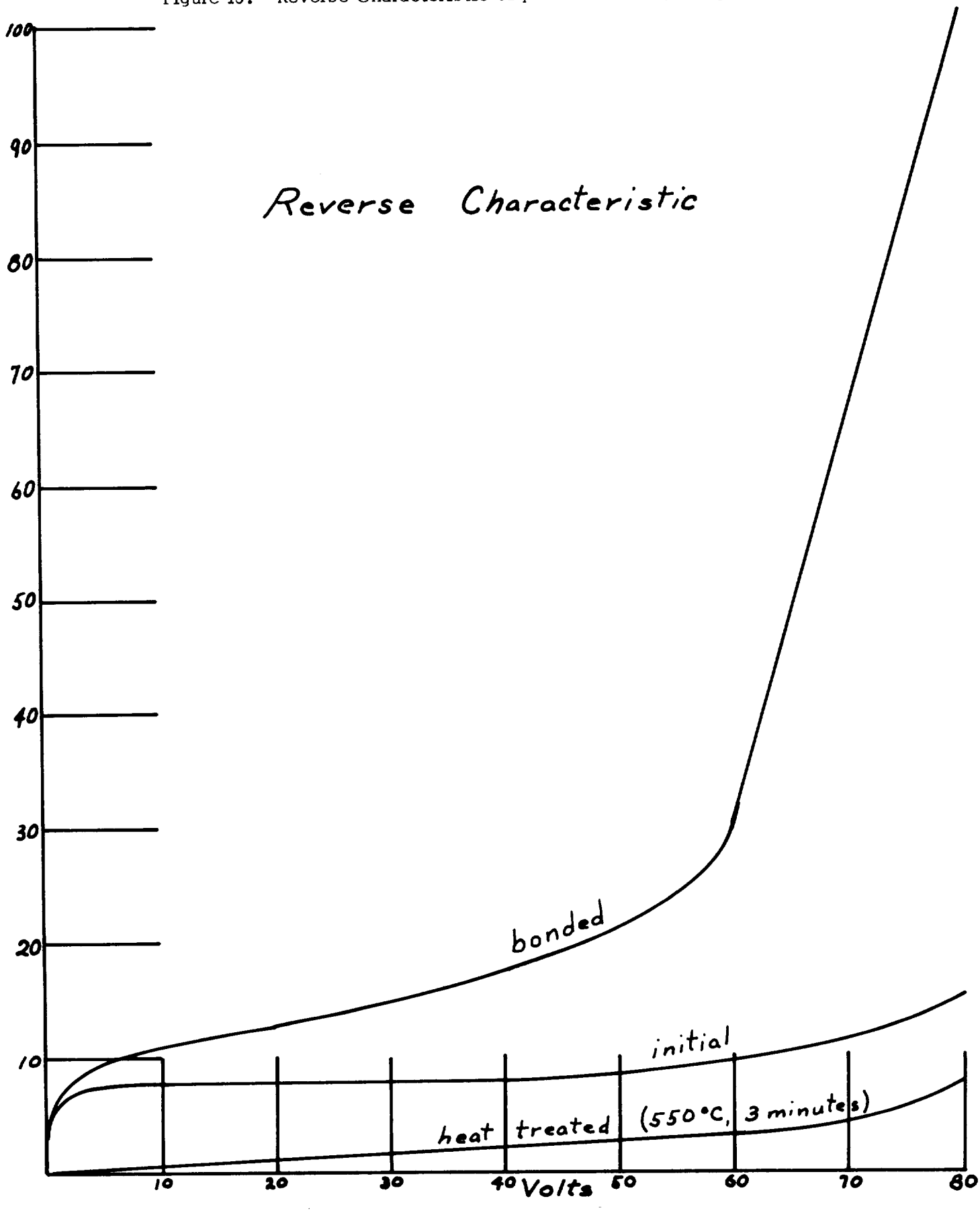

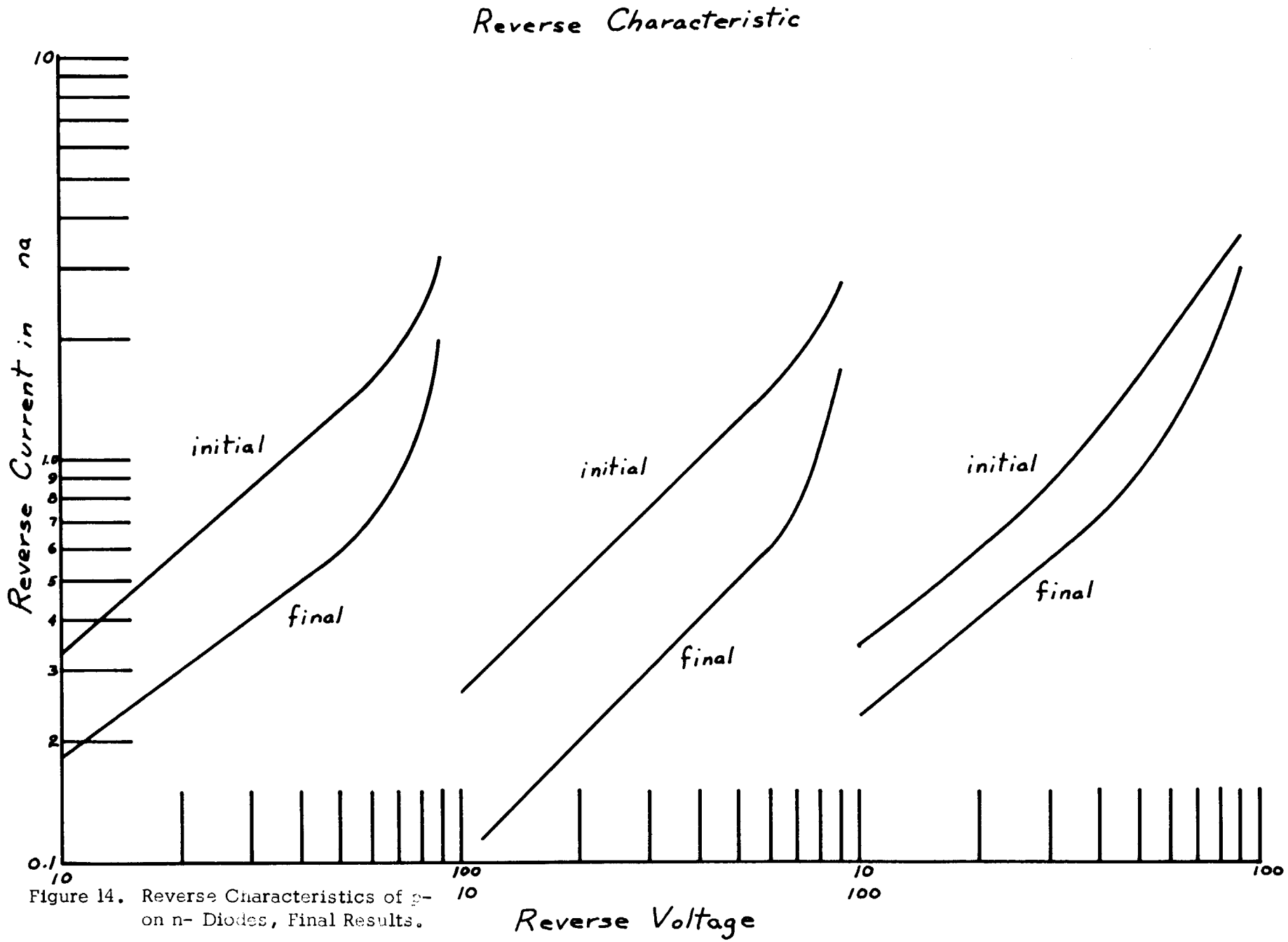

Figure 14. Reverse Characteristics of p-on n- Diodes, Final Results.

Figure 15. Reverse Characteristics of n- on p- Diodes.

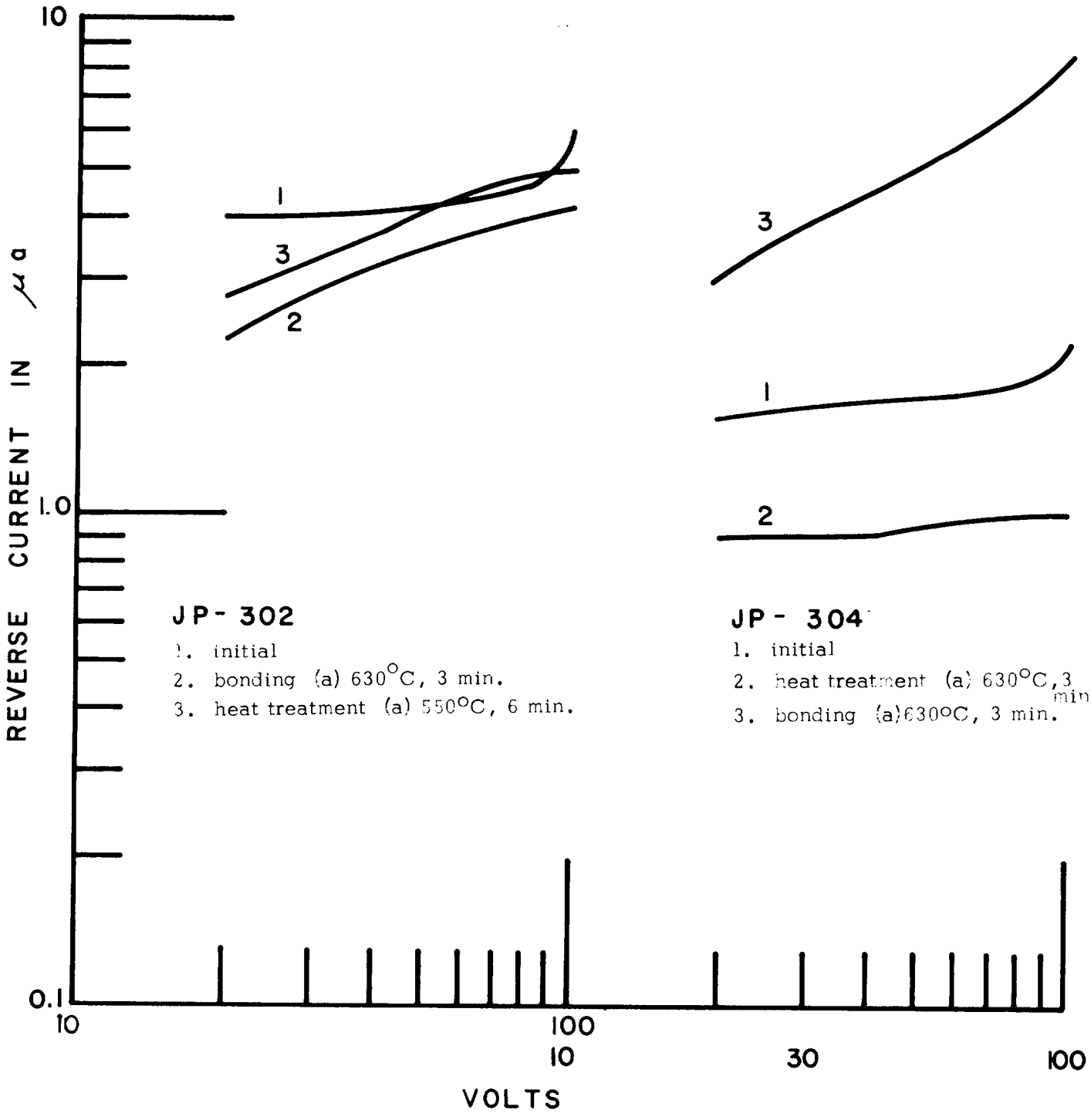

Figure 16. Channel Conductance versus Bias.

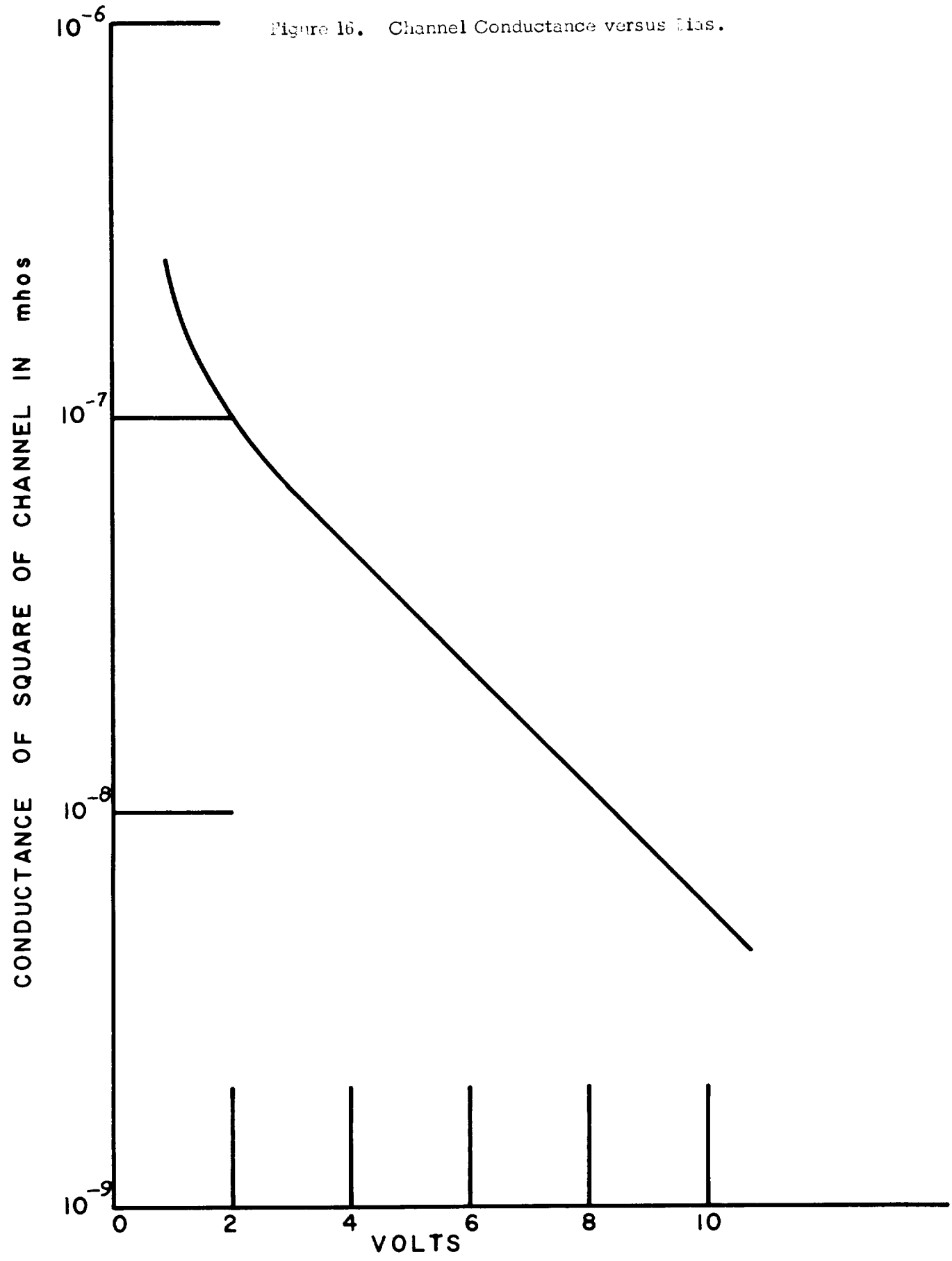

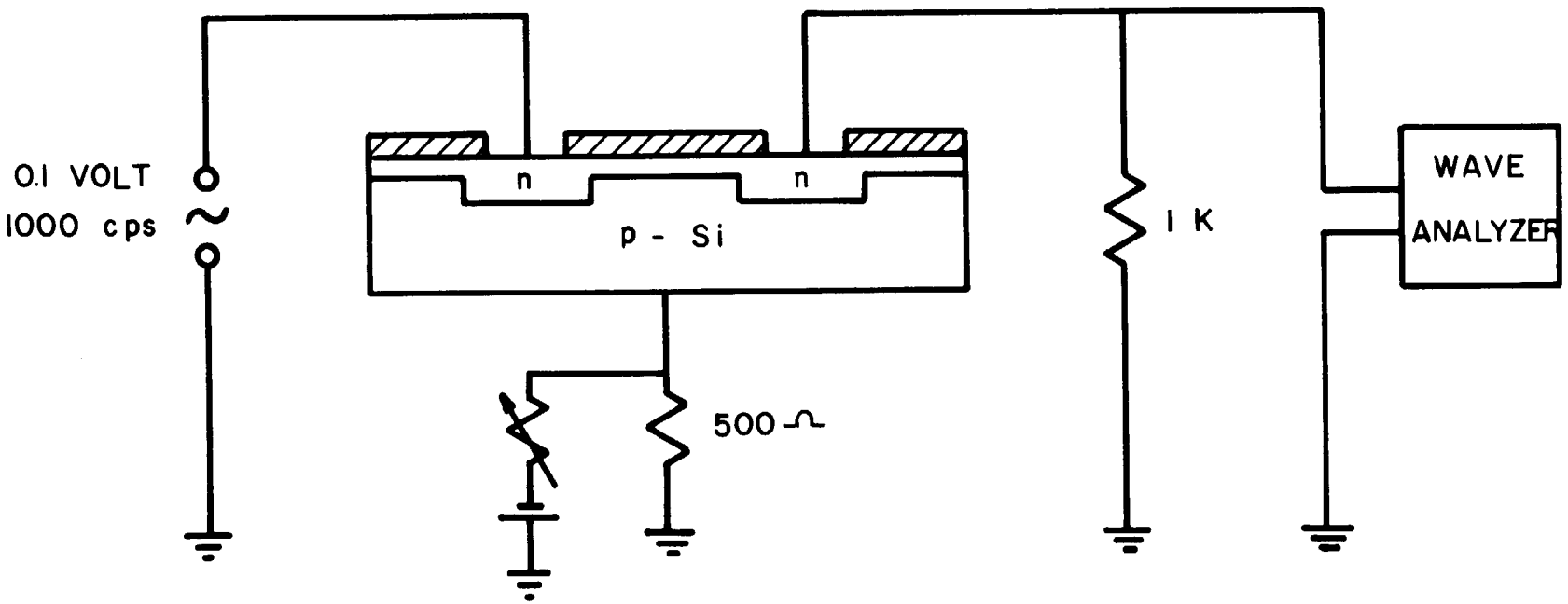

Figure 17. Circuit for Channel Conductance Measurements.